

Ergodicity breaking, ageing, and confinement in generalized diffusion processes with position and time dependent diffusivity

This content has been downloaded from IOPscience. Please scroll down to see the full text.

View [the table of contents for this issue](#), or go to the [journal homepage](#) for more

Download details:

IP Address: 129.187.254.46

This content was downloaded on 15/05/2015 at 09:16

Please note that [terms and conditions apply](#).

Ergodicity breaking, ageing, and confinement in generalized diffusion processes with position and time dependent diffusivity

Andrey G Cherstvy¹ and Ralf Metzler^{1,2}

¹ Institute for Physics and Astronomy, University of Potsdam,
D-14476 Potsdam, Germany

² Physics Department, Tampere University of Technology, FI-33101 Tampere,
Finland

E-mail: rmetzler@uni-potsdam.de and a.cherstvy@gmail.com

Received 5 February 2015

Accepted for publication 13 March 2015

Published 15 May 2015

Online at stacks.iop.org/JSTAT/2015/P05010

[doi:10.1088/1742-5468/2015/05/P05010](https://doi.org/10.1088/1742-5468/2015/05/P05010)

Abstract. We study generalized anomalous diffusion processes whose diffusion coefficient $D(x, t) \sim D_0|x|^{\alpha}t^{\beta}$ depends on both the position x of the test particle and the process time t . This process thus combines the features of scaled Brownian motion and heterogeneous diffusion parent processes. We compute the ensemble and time averaged mean squared displacements of this generalized diffusion process. The scaling exponent of the ensemble averaged mean squared displacement is shown to be the product of the critical exponents of the parent processes, and describes both subdiffusive and superdiffusive systems. We quantify the amplitude fluctuations of the time averaged mean squared displacement as function of the length of the time series and the lag time. In particular, we observe a weak ergodicity breaking of this generalized diffusion process: even in the long time limit the ensemble and time averaged mean squared displacements are strictly disparate. When we start to observe this process some time after its initiation we observe distinct features of ageing. We derive a universal ageing factor for the time averaged mean squared displacement containing all information on the ageing time and the measurement time. External confinement is shown to alter the magnitudes and statistics of the ensemble and time averaged mean squared displacements.

Keywords: diffusion



Contents

1. Introduction	2
2. Observables	3
3. Generalized diffusion processes	6
3.1. Unconfined motion	6
3.2. Ageing motion	10
3.3. Confined motion	12
3.3.1. Ageing and confined SBM	14
4. Discussion and outlook	15
Acknowledgments	17
References	17

1. Introduction

Deviations from Brownian motion are quite ubiquitous in a large variety of complex systems. Mostly such anomalous diffusion processes are characterized by a scaling form of the mean squared displacement (MSD),

$$\langle x^2(t) \rangle \sim t^\kappa. \quad (1)$$

The magnitude of the anomalous scaling exponent κ distinguishes subdiffusion for $0 < \kappa < 1$ and superdiffusion $\kappa > 1$ [1–4]. Examples for anomalous include the relative diffusion of tracers particles in fully turbulent [5] or weakly chaotic [6] systems as well as in groundwater aquifers [7]. Subdiffusion of charge carriers in amorphous semiconductors was originally analysed some 40 years ago [8] but is now regaining attention in the study of polymeric semiconductors [9]. However, the main current impetus for the study of anomalous diffusion processes is due to modern spectroscopic tools such as fluorescence correlation spectroscopy [10] and single particle tracking of submicron particles [11]. By these methods pronounced deviations from normal diffusion ($\kappa = 1$) were found in structured and crowded liquids [12–15] and in living biological cells [16–18]. Similarly, anomalous diffusion is observed in supercomputer studies of, inter alia, flexible networks [19] and lipid membranes [20].

The non-Brownian scaling of the MSD of the tracer particles may originate from a range of physical mechanisms. These include the subdiffusive motion on geometric fractals such as percolation clusters close to criticality [3, 18, 21] or the anomalous diffusion in Lorentz gases [22]. Another important class of anomalous diffusion models are continuous time random walks (CTRWs), in which the test particle's motion is interrupted by random

waiting times [23]. If the distribution of these waiting times is scale free, subdiffusion emerges [8], a phenomenon closely related to quenched trap models with exponentially distributed trap depths [1, 24]. The third class represents processes, in which the particle is driven by fractional Gaussian noise which is long range temporally correlated: the fractional Brownian motion [25] or associated fractional Langevin equation motion [26] are connected to viscoelastic environments [27] and represent the motion of tagged monomers in a Rouse chain [28] or a tracer particle in a single file [29]. A more complete overview of anomalous diffusion models provides [4].

Here we deal with the remaining class of popular stochastic models, in which the diffusion anomaly stems from the explicit position or time dependence of the diffusion coefficient. Modelling anomalous diffusion via a coordinate dependent diffusivity goes back to Richardson's analysis of relative diffusion in turbulent flows with $\kappa = 3$ [5]. Systematic variations of the local diffusion coefficient in space were, for instance, demonstrated in the cytoplasm of living biological cells [30]. A series of publications recently explored the stochastic properties of such heterogeneous diffusion processes (HDPs) [31–36]. Instead of the position dependence, Batchelor introduced a time dependent diffusion coefficient for the description of Richardson diffusion [37]. The generalization of Batchelors' process, Scaled Brownian motion (SBM) with a power law form for the diffusivity is very popular in the phenomenological description of anomalous diffusion [38]. Its stochastic properties were analysed in detail in [31, 39–43]. SBM was shown to grasp essential features of granular gases in the homogeneous cooling phase [44].

Physically, although both are truly Markovian processes HDPs and SBM are quite different in nature: HDPs are processes with a *multiplicative noise* [31, 32] while the time dependence of the diffusion coefficient in SBM heralds its fundamentally non-stationary character. Indeed experimentally it is often not possible to separate the effects of time and position variation of the diffusivity—compare, for instance, the data in [45]. This poses the question how exactly the position and time dependence of the diffusion coefficient built into HDPs and SBM conspire. How do they compete with each other? On the level of the stochastic Langevin we here analyse in detail generalized diffusion processes (GDPs) with the both the position and time dependent diffusion coefficient³

$$D(x, t) \sim (1 + \beta)D_0|x|^{\alpha}t^{\beta}, \quad (2)$$

where the physical dimension of the prefactor D_0 is $[D_0] = \text{cm}^{2-\alpha}\text{s}^{-1-\beta}$. The choice (2) thus combines the two parent processes (HDP and SBM) multiplicatively. In particular, we derive the ensemble and time averaged MSDs as well as their statistical properties. We also analyse the ageing behaviour and the effects of external confinement. We will discuss similarities and disparities with other anomalous stochastic processes.

2. Observables

We start by introducing the physical observables, that we are going to analyse in the remainder of this work. The most standard quantity to classify a stochastic process is the

³ Indeed, for turbulent diffusion, both position and time dependence of the diffusivity was considered earlier in the context of Richardson diffusion in [46].

MSD (1), which is defined in terms of the spatial average

$$\langle x^2(t) \rangle = \int x^2 P(x, t) dx \quad (3)$$

over the available space region, where $P(x, t)$ is the probability density function to find the test particle at position x at time t . This is typically a good measure when many short trajectories of tracer particles are available. In many single particle tracking experiments, however, few long time traces $x(t)$ of length T (the measurement time) are available. The time series $x(t)$ is usually evaluated in terms of the time averaged MSD

$$\overline{\delta^2(\Delta)} = \frac{1}{T - \Delta} \int_0^{T-\Delta} [x(t + \Delta) - x(t)]^2 dt, \quad (4)$$

where Δ is the lag time. Often, the additional average

$$\langle \overline{\delta^2(\Delta)} \rangle = \frac{1}{N} \sum_{i=1}^N \overline{\delta_i^2(\Delta)} \quad (5)$$

over an ensemble of N individual trajectories is taken to produce smooth results.

For Brownian motion, the increments are stationary, and the time averaged MSD in the limit of long times becomes identical to the ensemble MSD: $\lim_{T/\Delta \rightarrow \infty} \overline{\delta^2(\Delta)} = \langle x^2(\Delta) \rangle$ [4, 47–49]. Due to this identity we call Brownian motion an ergodic process [50]. The same is true for anomalous diffusion processes driven by fractional Gaussian noise [26, 51, 52] (although pronounced transients may become relevant [15, 53]), as well as for diffusion on fractals [54]. In contrast, non-stationary processes are subject to the disparity

$$\lim_{T/\Delta \rightarrow \infty} \overline{\delta^2(\Delta)} \neq \langle x^2(\Delta) \rangle. \quad (6)$$

This behaviour is referred to as *weak ergodicity breaking* [4, 47–49, 55–58]. For a range of anomalous diffusion processes, the time averaged MSD in the limit $\Delta \ll T$ was found to scale *linearly* in the lag time,

$$\langle \overline{\delta^2(\Delta)} \rangle \simeq \frac{\Delta}{T^{1-\kappa}}, \quad (7)$$

despite the anomalous scaling of the ensemble averaged MSD (1). Simultaneously, the explicit dependence on the measurement time shows that the process is progressively slowing down ($0 < \kappa < 1$) or picking up speed ($\kappa > 1$). The specific form (7) was derived, inter alia, for subdiffusive continuous time random walks [56–58], HDPs [31, 32], and SBM [31, 40, 41] diffusion processes. We note that a similar linear lag time dependence of the time averaged MSD was also observed in ultraslow processes with a logarithmic form of the ensemble averaged MSD [43, 59–62].

Ergodic processes are reproducible in the sense that each time we evaluate some observables—for a sufficiently long measured time series—we obtain the same result with only minor deviations. Quantified in terms of the dimensionless variable [58]

$$\xi(\Delta) = \frac{\overline{\delta^2(\Delta)}}{\langle \overline{\delta^2(\Delta)} \rangle} \quad (8)$$

this means that the associated distribution $\phi(\xi)$ converges to the delta function, $\lim_{T/\Delta \rightarrow \infty} \phi(\xi) = \delta(\xi - 1)$ [4, 47, 48, 58]. Weakly non-ergodic processes have different limit distributions for $\phi(\xi)$ for sufficiently long time series. For instance, subdiffusive continuous

time random walks have a finite value $\phi(\xi = 0)$ and a distinct contribution away from the ergodic value $\xi = 1$ [4, 47, 48, 58]. HDPs have shapes of $\phi(\xi)$ that are similar to Gamma distributions with $\phi(\xi = 0) = 0$ [32]. SBMs are weakly non-ergodic but asymptotically reproducible [40, 41].

The spread of the time averaged MSD at given lag time $\Delta \ll T$ is quantified by the ergodicity breaking parameter [4, 47, 48, 58]

$$\text{EB}(\Delta) = \langle \xi^2(\Delta) \rangle - \langle \xi(\Delta) \rangle^2 = \langle \xi^2(\Delta) \rangle - 1. \quad (9)$$

For Brownian motion EB vanishes linearly with Δ/T [4],

$$\lim_{\Delta/T \rightarrow 0} \text{EB}_{\text{BM}}(\Delta) = \frac{4\Delta}{3T}. \quad (10)$$

Sometimes, the alternative ergodic parameter

$$\mathcal{EB}(\Delta) = \frac{\langle \overline{\delta^2(\Delta)} \rangle}{\langle x^2(\Delta) \rangle} \quad (11)$$

is invoked to provide some additional information about the ergodic properties of the process [4, 63]. The ergodicity breaking parameter (9) for any finite ratio Δ/T for non-ergodic processes is larger than the corresponding Brownian value (10) and may not vanish in the limit of long measurement times. As we show below the ergodicity breaking parameter (9) is a sensitive measure for the physical processes generating a given anomalous diffusion process. Other observables such as the ensemble and time averaged MSDs often feature similar or even identical functional forms for different processes and are thus not suitable to discern a specific process, compare the discussion in [4, 64, 65].

Finally, we address the ageing behaviour of the anomalous diffusion processes. This is the explicit dependence of physical observables on the ageing time t_a elapsing between the initiation of the process at $t = 0$ and the start of the measurement at t_a . In particular, for the time averaged MSD of the aged system the evaluation of the associated time series is then performed in terms of

$$\overline{\delta^2(\Delta; t_a)} = \frac{1}{T - \Delta} \int_{t_a}^{t_a + T - \Delta} [x(t + \Delta) - x(t)]^2 dt. \quad (12)$$

For subdiffusive continuous time random walk processes [66], HDPs [35], and SBM [42], it was found that the aged and non-aged time averaged MSDs for $\Delta \ll T$ fulfil the relation

$$\langle \overline{\delta^2(\Delta; t_a)} \rangle = \Lambda_\kappa \left(\frac{t_a}{T} \right) \langle \overline{\delta^2(\Delta; 0)} \rangle \quad (13)$$

and thus differ only by the ageing factor

$$\Lambda_\kappa \left(\frac{t_a}{T} \right) \approx \left(1 + \frac{t_a}{T} \right)^\kappa - \left(\frac{t_a}{T} \right)^\kappa \quad (14)$$

containing, multiplicatively, all information on the ageing and measurement times.

In what follows, we analyse these quantities in detail for the GDP composed of the HDP and SBM parent diffusion processes.

3. Generalized diffusion processes

Based on the spatio-temporal dependence (2) of the diffusion coefficient we define the generalized diffusion process in terms of the overdamped Langevin equation

$$\frac{dx(t)}{dt} = \sqrt{D(x,t)} \times \xi(t). \quad (15)$$

The noise $\xi(t)$ is Gaussian with unit variance and zero mean [32, 41]. For the position coordinate $x(t)$, this is a multiplicative equation, which we extensively tested for HDPs [32–35]. With respect to the time dependence of $D(x,t)$, we analysed this Langevin equation in the context of SBM processes [41].

We interpret the Langevin equation in the Stratonovich sense. In the mid-point discrete version, the particle displacement in the $(i+1)$ st step thus becomes [32]

$$x_{i+1} - x_i = \sqrt{2 \left[D \left(\frac{x_{i+1} + x_i}{2}, t_i \right) + D_{\text{off}} \right]} \times (y_{i+1} - y_i), \quad (16)$$

where the increments $(y_{i+1} - y_i)$ of the Wiener process represent a δ -correlated Gaussian noise with unit variance. Unit time intervals separate the consecutive iteration steps. To avoid a trapping of particles in the regions of zero diffusivity for certain exponents for α and β , the form (16) chosen for the simulations was regularized by addition of the small constant $D_{\text{off}} = 10^{-3}$, compare [32, 34, 35] for more details on the simulation procedure. The particle's initial starting position in all the results presented below is $x_0 = 0.1$ (see [35] for details of the effects of x_0) and $D_0 = 0.01$. The discrete scheme (16) is supplied with either natural or reflective boundary conditions in the following.

From the Langevin equation (15) it is straightforward to derive the diffusion equation (compare [32])

$$\frac{\partial}{\partial t} P(x,t) = \frac{\partial}{\partial x} \left[\sqrt{D(x,t)} \frac{\partial}{\partial x} \left(\sqrt{D(x,t)} P(x,t) \right) \right]. \quad (17)$$

Following the Stratonovich interpretation we see that the diffusion coefficient appears symmetric with respect to the Laplacian operator. In the limits $\beta \rightarrow 0$ and $\alpha \rightarrow 0$, respectively, we recover the diffusion equations with purely position dependent [32] and time dependent [41] diffusivity.

3.1. Unconfined motion

For unconfined motion we apply the natural boundary conditions $\lim_{|x| \rightarrow \infty} P(x,t) = 0$ to the GDP diffusion equation (17) to find the probability density function

$$P(x,t) = \frac{|x|^{1/p-1}}{\sqrt{4\pi D_0 t^{1+\beta}}} \exp \left(-\frac{|x|^{2/p}}{(2/p)^2 D_0 t^{1+\beta}} \right), \quad (18)$$

where we used the abbreviation

$$p = \frac{2}{2-\alpha}. \quad (19)$$

The functional form of the probability density function (18) thus combines the spatial features of the HDP process with the space dependence $\simeq |x|^\alpha$ of the diffusivity [32] and the modified time dependence due to the contribution $\simeq t^\beta$ of the diffusivity of

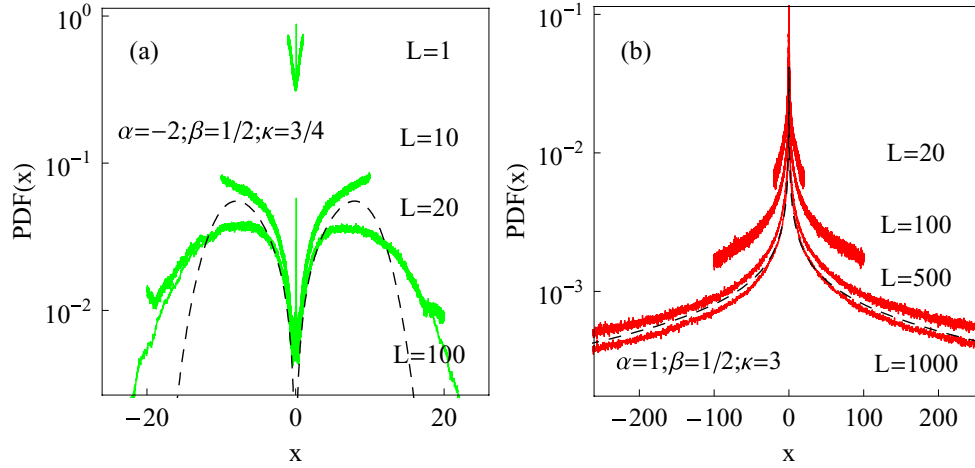


Figure 1. Probability density function $P(x,t)$ for nearly free and confined (see below) GDPs for (a) subdiffusive and (b) superdiffusive choices of the critical exponents α and β , as indicated in the plots. The analytical result for the probability density function from equation (18) for unconfined GDP motion are the dashed lines. For subdiffusive GDPs the small spike at $x = 0.1$ is a remainder of the initial starting position of the particles. For superdiffusive GDPs this is not visible due to the fast formation of the peak of $P(x,t)$ at $x = 0$ in the region of the slowest diffusivity. Parameters: $T = 10^4$, $N = 10^3$, $D_0 = 0.01$. The L values are as indicated.

SBMs [41]. In particular, for $p > 1$ ($p < 1$) we observe a stretched (compressed) Gaussian shape for larger x as well as a cusp (dip to zero) close to the origin. This behaviour is supported by simulations presented in figure 1, revealing a particularly good agreement with equation (18) for superdiffusive GDPs. In the subdiffusive case significantly longer simulations would be necessary than we can access with our current numerical setup.

Integration based on equation (18) produces the ensemble averaged MSD

$$\langle x^2(t) \rangle = \frac{\Gamma(1/2 + p)}{\pi^{1/2}} \left(\frac{2}{p}\right)^{2p} (D_0 t^{1+\beta})^p. \quad (20)$$

The scaling exponent

$$\kappa = (1 + \beta)p \quad (21)$$

is thus given by the product of the HDP and SBM exponents. In the limits $\beta = 0$ and $\alpha = 0$ we recover the scaling exponents $\kappa = p$ and $\kappa = 1 + \beta$ of the pure parent processes for HDP and SBM, respectively [31, 32, 41]. For the parameter range $-2 < \alpha < 2$ and $-1 < \beta < 1$ of the HDP and SBM processes, the phase space of the GDP is depicted in figure 2: for all parameter values in the red (blue) areas, the GDP is superdiffusive (subdiffusive). Note that we also simulated the GDPs for the temporal exponent $\beta = 3/2$ outside of the typical SBM range $-1 < \beta < 1$, see figure 3(a), observing good agreement with the prediction for the MSDs (20) and (22).

In analogy to the derivations in [32, 41], we obtain the time averaged MSD in the limit $\Delta \ll T$,

$$\langle \overline{\delta^2(\Delta)} \rangle \sim \frac{\Gamma(1/2 + p)}{\pi^{1/2}} \left(\frac{2}{p}\right)^{2p} D_0^p \frac{\Delta}{T^{1-(1+\beta)p}} \quad (22)$$

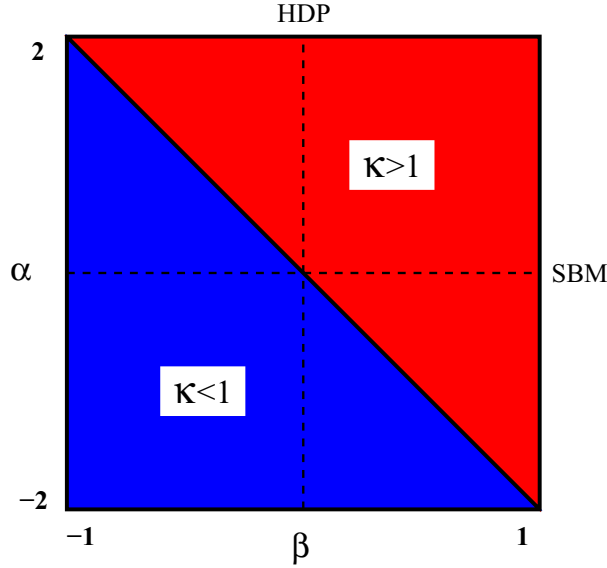


Figure 2. Phase space of the generalized diffusion process. In the red (blue) areas the GDP is superdiffusive (subdiffusive). The dashed lines at $\alpha = 0$ ($\beta = 0$) represent pure SBM (HDP), respectively.

or

$$\langle \overline{\delta^2(\Delta)} \rangle \sim \langle x^2(\Delta) \rangle \left(\frac{\Delta}{T} \right)^{1-(1+\beta)p}. \quad (23)$$

Time and ensemble averages are thus disparate, and in analogy to the parent processes HDP and SBM we observe weak ergodicity breaking. The alternative ergodicity breaking parameter for the GDP thus becomes

$$\mathcal{EB}(\Delta) \sim \left(\frac{\Delta}{T} \right)^{1-(1+\beta)p}. \quad (24)$$

The explicit dependence on the measurement time T in relations (22) and (24) is a signature of the non-stationary character of the GDP. As function of T the amplitude of the time averaged MSD continuously decreases (increases) for subdiffusive (superdiffusive) parameters, see figure 4. This figure shows the time averaged MSD from simulations for a range of values of the scaling exponents α and β . The predicted scaling $\langle \overline{\delta^2(T)} \rangle \simeq T^{(1+\beta)p-1}$ according to equation (22) agrees nicely with the simulated data. The linear lag time dependence $\langle \overline{\delta^2(\Delta)} \rangle \simeq \Delta$ is supported by the simulations shown in figure 3 and below in figure 8.

Note that for those combinations of the scaling exponents α and β for which the ensemble MSD grows linearly ($\kappa = 1$, see the diagonal separating subdiffusion and superdiffusion in figure 2) the GDP is still weakly non-ergodic, as illustrated by the irreproducibility of the individual time averaged MSDs and their inequivalence with the ensemble MSD shown in figure 3(b) for $\alpha = 1$ and $\beta = -1/2$. Despite the fact that the trends of the spatial and temporal variation of the GDP diffusivity compensate each other in terms of the MSD the overall process is still non-stationary.

The scatter of the time averaged MSD from individual simulated trajectories is a sensitive function of the diffusivity $D(x, t)$, as shown in figure 5. This figure contains the

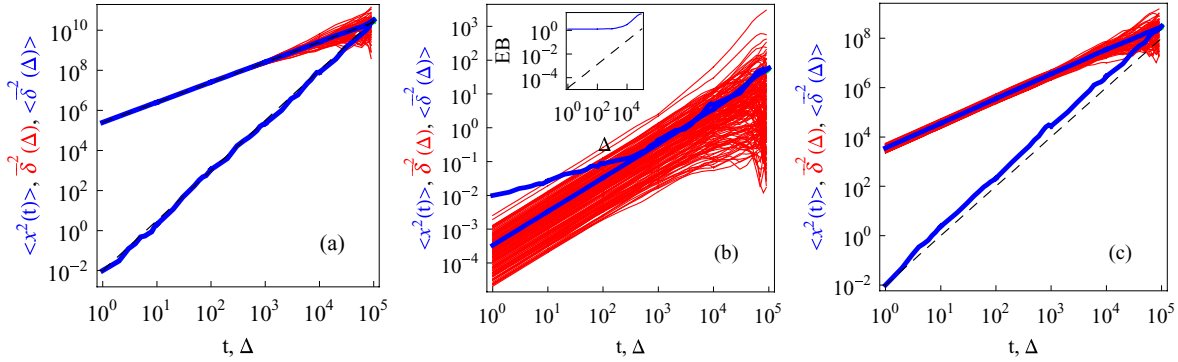


Figure 3. (a) Ensemble and time averaged MSDs for unconfined GDPs for $\alpha = -1/2$, $\beta = 3/2$, $T = 10^5$, and $N = 100$. (b) Ensemble and time averaged MSDs of unconfined GDPs with $\alpha = 1$ and $\beta = -1/2$, that is, for a linear time dependence of the ensemble MSD ($\kappa = 1$). Note the initial relaxation of the ensemble MSD to the asymptotic behaviour $\langle x^2(t) \rangle \sim t^1$. The inset shows the behaviour of the ergodicity breaking parameter with the Brownian asymptote (10), shown as the dashed line. (c) Ensemble and time averaged MSDs for unconfined SBM process for $\beta = 3/2$. The limiting laws (20) and (22) in panels (a) and (c) are shown by the dashed curves. Parameters: $T = 10^5$, $N \sim 50$.

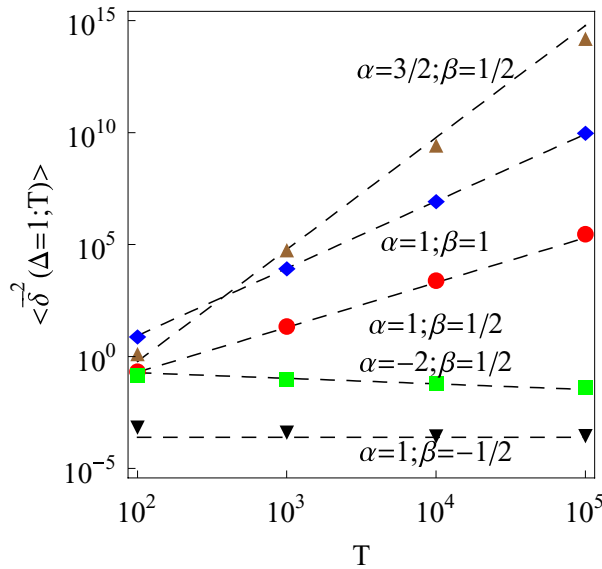


Figure 4. Time averaged MSD for GDPs in the limit $\Delta/T \ll 1$ ($\Delta = 1$). The asymptotes are given by equation (23) and the values of the exponents α and β are as indicated. Good agreement with the predicted scaling behaviour is observed.

results both for nearly unconfined and confined GDPs. For subdiffusive GDPs, for instance the case $L = 100$ can effectively be considered as a free process within the simulation time: most of the traces do not reach the reflecting boundary during the simulated $T = 10^5$ steps, see the top row of figure 8. The spread of δ^2 becomes broader as the value of the spatial exponent α approaches its critical value $\alpha \rightarrow 2$ (not shown). This is a characteristic

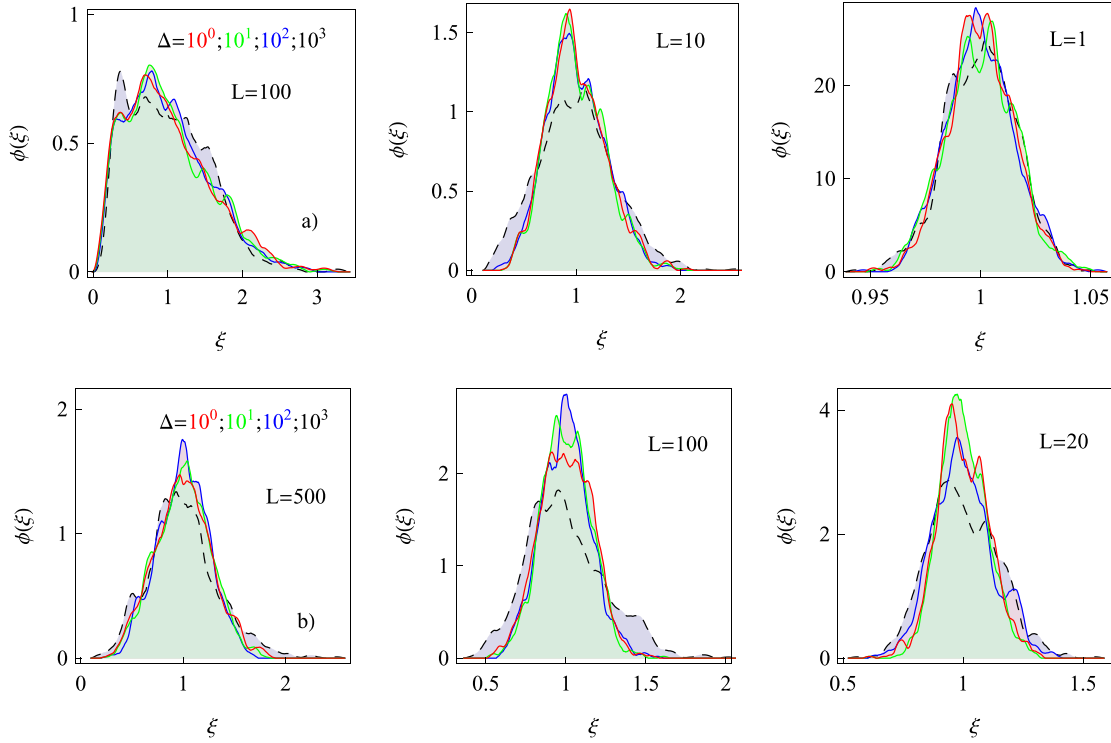


Figure 5. Amplitude scatter distribution $\phi(\xi)$ of individual time averaged MSD traces of the GDP for varying lag times Δ and the extent of confinement. As parameters we chose $T = 10^4$, $N = 10^3$, as well as for the top row $\alpha = -2$ and $\beta = 1/2$ (subdiffusion), for the bottom row $\alpha = 1$, $\beta = 1/2$ (superdiffusion). Different degrees of confinement were imposed, the left panel in top row corresponds to effectively free motion.

property of HDPs [35]. With increasing Δ the spread of $\overline{\delta^2}$ traces increases only slightly. For subdiffusive GDPs the distribution $\phi(\xi)$ is similar to the asymmetric Rayleigh form discussed in [32].

The ergodicity breaking parameter $EB(\Delta)$ of GDPs is illustrated in figure 6(a). The deviations from the Brownian result (10) in the limit $\Delta/T \ll 1$ quantifies the departure of the diffusing particles from the ergodic behaviour. We find that for GDPs the value of the ergodicity breaking parameter does not vanish in the limit $\Delta/T \ll 1$, see figure 6(a). For GDPs the value of EB in the limit $\Delta/T \rightarrow 0$ varies significantly with β , as shown in figure 6(c). We note that the diffusing particles under lesser confinement produce larger values of EB , compare the curves in figure 6(a), see below. We also note that varying initial conditions x_0 alter the values of EB (not shown). The auxiliary ergodicity breaking parameter for free and confined GDP motion is shown in figure 6(b) together with the asymptotes (24).

3.2. Ageing motion

The effect of ageing, that is, the dependence of physical observables on the time difference t_a between system initiation at $t = 0$ and start of the measurement of the process in

Ergodicity breaking, ageing and confinement in generalized diffusion processes

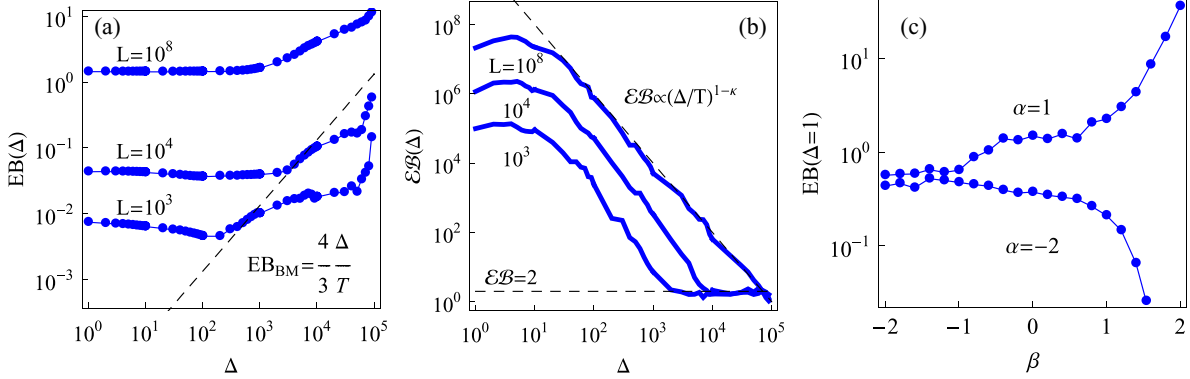


Figure 6. Ergodicity breaking parameters EB (panel *a*) and \mathcal{EB} (panel *b*) for free ($L = 10^8$) and confined superdiffusive GDPs ($\beta = 1$, $\alpha = 1/2$). The asymptotes (10) for Brownian motion in (*a*) and (24) in (*b*) are shown as the dashed lines. The values of the confinement L are as indicated. Parameters: $T = 10^5$, $N = 150$. (Panel *c*): log-linear plot of EB at $\Delta = 1$ for different β values for free GDPs. Parameters: $T = 10^4$, $N = 500$.

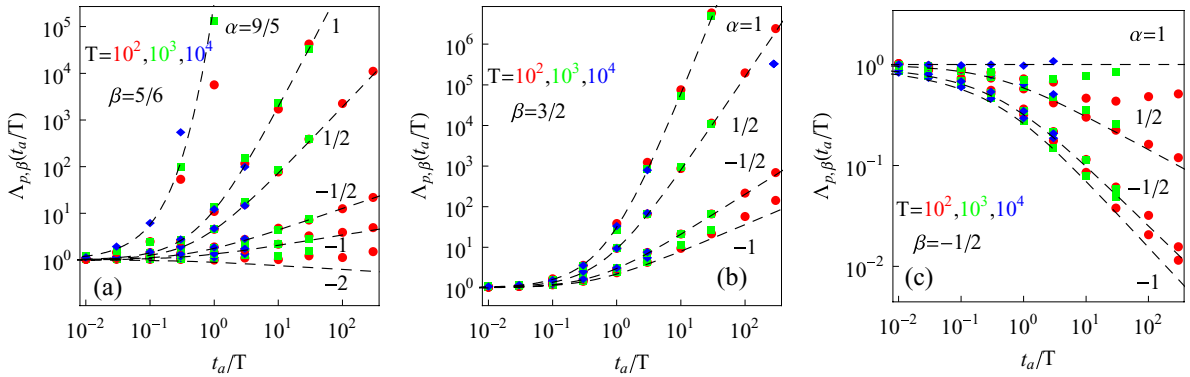


Figure 7. Ageing factor $\Lambda_{p,\beta}(t_a/T)$ for aged GDPs in the limit $\Delta/T \ll 1$ ($\Delta = 1$). The values of α are given in the plots. We show the values $\beta = 5/6$ (panel *a*), $\beta = 3/2$ (panel *b*), and $\beta = -1/2$ (panel *c*). The asymptotes (25) are represented by the dashed lines. Parameters: the overall length of the traces is 10^5 steps, of which the evaluated trace lengths T are indicated in the plots. We averaged over $N = 200$ traces for each data point.

analogy to the results for HDPs [35] and SBM [42] factorizes according to equation (13). The ageing factor (14)

$$\Lambda_{p,\beta} \left(\frac{t_a}{T} \right) \sim \left(1 + \frac{t_a}{T} \right)^{p(1+\beta)} - \left(\frac{t_a}{T} \right)^{p(1+\beta)} \quad (25)$$

now has a parametric dependence on both $p = 2/(2 - \alpha)$ and β . This scaling with the ageing time is indeed supported by our computer simulations for a number of combinations of the scaling exponents α and β , as shown in figure 7. Figure 7(*b*) shows that for aged GDPs the scaling function (25) remains valid also for $\beta > 1$, see the discussion for ageing SBM below. Note that for subdiffusive GDPs in general longer traces are needed to obtain the same degree of convergence to equation (25), as detailed in figure 7(*c*).

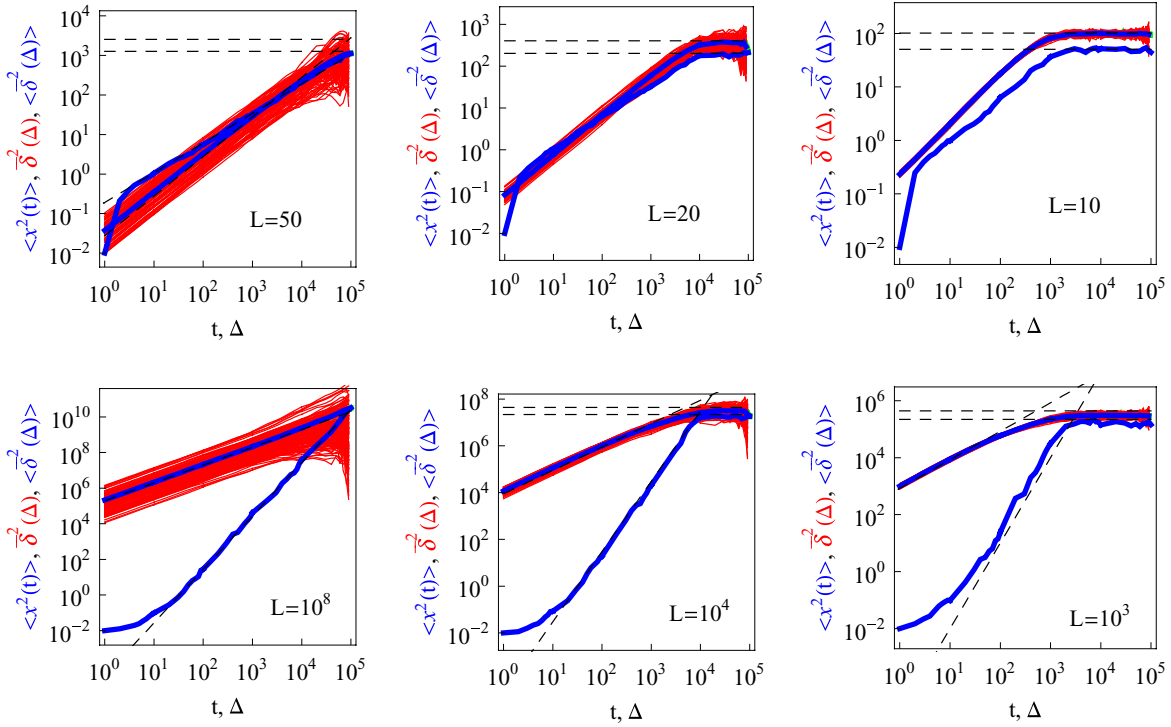


Figure 8. Ensemble and time averaged MSDs for confined subdiffusive ($\alpha = -2$ and $\beta = 1/2$, top row) and superdiffusive ($\alpha = 1$ and $\beta = 1/2$, bottom row) GDPs. These exponents are the same as used in figure 5. The limiting behaviours (20) and (22) for unconfined motion as well as the plateau value (26) under confinement are indicated by the dashed curves. Parameters: $T = 10^5$ and $N = 150$. The width of the confining interval L is indicated in the panels, the value $L = 10^8$ corresponds to an effectively unconfined situation.

3.3. Confined motion

Let us now address GDPs in the confinement of hard walls. To this end we establish reflecting boundary conditions at $x = \pm L$. Figure 8 demonstrates that for weak confinement (large L values) and at shorter (lag) times the ensemble and time averaged MSDs behave similarly to those of the unconfined process, as expected. At stronger confinement and at longer (lag) times the MSD saturates at the plateau value

$$\langle x^2 \rangle_{\text{st}} \sim p^{-3/5} L^2 / 3. \quad (26)$$

The α -dependence of the value (26) in the prefactor $p^{-3/5}$ reflects the fact that the associated stationary probability density function is still position dependent due to the variation of the diffusivity, see also figure 1. For $\alpha = 0$, the process assumes an equidistribution with the value $1/(2L)$. We stress that the plateau value (26) is independent of the temporal scaling exponent β . In the hard confinement by infinitely steep walls the stationary state is generally independent of any x -independent noise strength. The variance (26) is thus geometry induced and not due to the competition of thermal noise and confinement as, for instance, in an harmonic confinement. In the latter case, no stationary solution is reached for SBM [41].

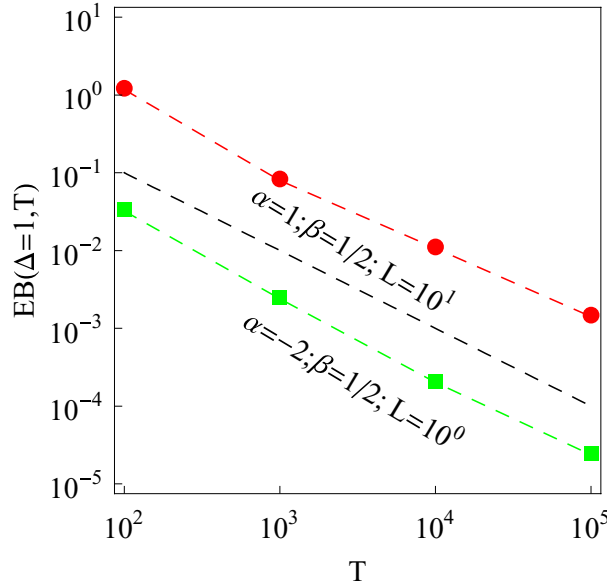


Figure 9. Ergodicity breaking parameter EB for confined GDPs from simulations. The asymptote (27) is indicated by the black dashed curve. Notations for the symbols are the same as in figure 4.

Figure 8 also shows that for the same interval width L subdiffusive GDPs require longer times to reach the stationary values. After reaching the stationary plateau, the value of the time averaged MSD is twice that of the ensemble MSD, an effect of the very definition of the time averaged MSD [4]. Note that due to the pole at $\Delta \rightarrow T$ in the definition (4) of the time averaged MSD the asymptotic equivalence $\lim_{\Delta \rightarrow T} \overline{\delta^2(\Delta)} \rightarrow \langle x^2(T) \rangle$ holds [4].

The probability density function $P(x, t)$ of confined GDPs for different values of the scaling exponents α and β as well as of varying degrees of confinement is shown in figure 1. It is seen that when the particle is reflected repeatedly in stronger confinement by the walls, the tails of $P(x, t)$ become perceivably raised, to fulfil the boundary condition $\partial P(x, t)/\partial x|_{x=0} = 0$.

The distribution of amplitudes of individual time averaged MSDs described by $\phi(\xi)$ for confined GDPs is shown in figure 5. The width of $\phi(\xi)$ decreases for more severe confinement, as expected. The width of $\phi(\xi)$ for shorter measurement times T is larger (not shown), due the smaller number of reflections from the walls. For confined GDPs $\phi(\xi)$ becomes more localized and symmetric both for subdiffusive and superdiffusive combinations of the scaling exponents α and β , as demonstrated in figure 5. As one may venture from figure 8, the spread of individual $\overline{\delta^2}$ decreases severely when extreme excursions of particles causing large trajectory-to-trajectory variations are progressively impeded by the confinement.

The dependence of the ergodicity breaking parameter on the lag time Δ for different interval lengths L is shown in figure 6(a), and the variation of EB with the measurement time T is illustrated in figure 9. We find for GDPs the reciprocal dependence in the limit of short lag times

$$\overline{\text{EB}}(T) \sim \frac{1}{T} \quad (27)$$

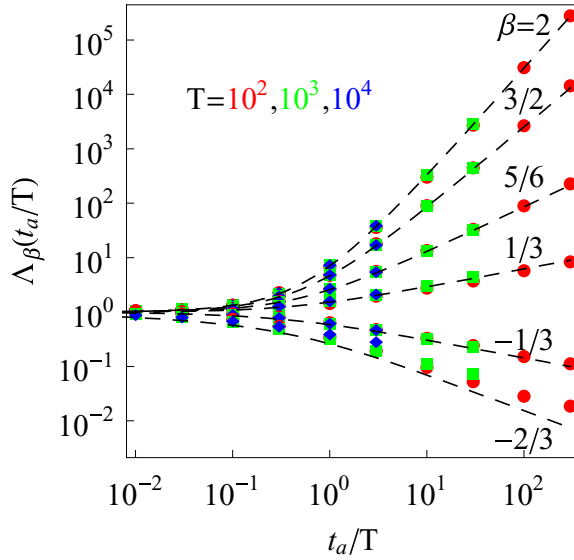


Figure 10. Ageing factor Λ_β for ageing SBM, the dashed lines represent the asymptote (25) for $p = 1$. Parameters: the total trajectory length is 10^5 steps and the length T is given in the plot. The averaging was over $N \approx 100$ trajectories for each β value, and we chose $\Delta = 1$.

with the trace length T , similar to the behaviour of confined HDPs [35]. Similar to HDPs and SBM, for free and confined GDPs our simulations confirm equation (24) in figure 6(b). In the long time limit the saturation plateau is reached and $\mathcal{EB}(\Delta) \rightarrow 2$. We point out that this behaviour is significantly different from that of subdiffusive continuous time random walks, for which the power-law $\langle \delta^2(\Delta) \rangle \simeq (\Delta/T)^{1-\alpha}$ is obtained [55].

3.3.1. Ageing and confined SBM. Let us briefly digress to study the behaviour under ageing and the confinement by hard walls of the pure SBM. From the results of [41] together with the definition of the ageing time averaged MSD (12) we find the full form of the ageing factor

$$\Lambda_\beta(t_a/T) = \frac{(1 + t_a/T)^{\beta+2} + (t_a/T)^{\beta+2} - (t_a/T + \Delta/T)^{\beta+2} - (1 + t_a/T - \Delta/T)^{\beta+2}}{1 - (\Delta/T)^{\beta+2} - (1 - \Delta/T)^{\beta+2}} \quad (28)$$

that for short ageing $t_a/T \ll 1$ and lag times $\Delta/T \ll 1$ reduces to relation (25) with $p = 1$. This implies that for superdiffusive SBM with $\beta > 0$ the magnitude of time averaged MSD increases with the ageing time t_a/T and decreases for subdiffusive SBM with $\beta < 0$, as shown in figure 10. Physically this is a consequence of the continued acceleration of particles in the superdiffusive case, contrasting the progressively localized particles for subdiffusion. We refer to [42] for more details on the properties of ageing SBM including the mean first passage time density.

We support the limiting form (25) with $p = 1$ of the ageing factor for ageing SBM from computer simulations in figure 10 for a range of scaling exponents β . The agreement of the simulations with the asymptote (25) is particularly good for the case of superdiffusive SBM with $T = 10^5$ steps. Strongly subdiffusive SBMs likely require longer traces to converge better to (25). Performing simulations for the range $\beta > 1$ we also reveal excellent agreement with the ageing factor (25), see the top curves in figure 10.

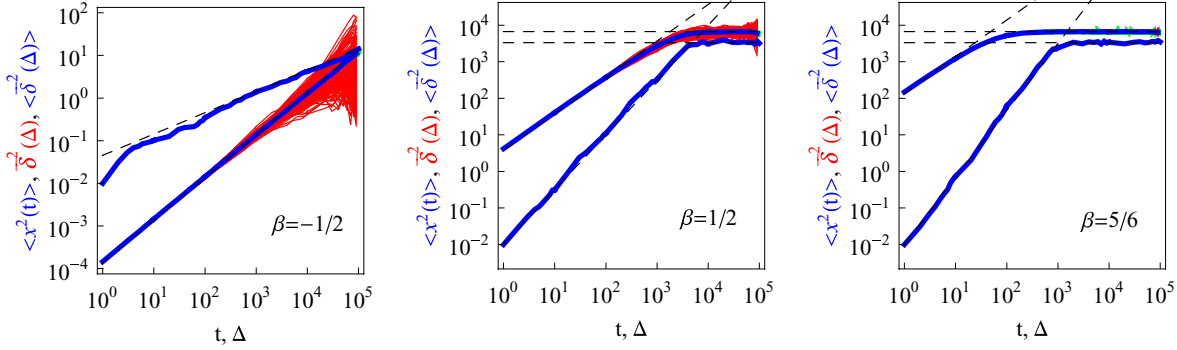


Figure 11. MSD and time averaged MSD for the SBM process confined on an interval. The values of β are indicated in the plots. The asymptotes for the unperturbed MSD, time averaged MSD, and the Brownian plateaus are the dashed lines. For $\beta = -1/2$ the confining boundaries are not reached. Parameters: $N = 150$, $T = 10^5$, $x_0 = 0.1$, $D_0 = 0.01$ and $L = 10^2$.

For SBM processes confined by an harmonic potential [41] even in the limit of long T the MSD continues to vary according to $\langle x^2(t) \rangle_{\text{st}} \sim t^\beta$ and does not relax to a plateau, due to the continuous variation of the diffusivity. This gives rise to an increasing (at $\beta > 0$) or decreasing ($\beta < 0$) MSD of the diffusing particles. Concurrently, an intermediate plateau $\langle \overline{\delta^2} \rangle_{\text{st}} = \text{const}$ exists for the time averaged MSD after the initial linear growth with the lag time Δ [41]. When confined between reflecting boundaries $-L < x < L$ —similar to the GDPs considered above—the MSD of the SBM reaches the Brownian plateau $L^2/3$, irrespective of the value of β , see figure 11. As β increases the particles reach the boundary $x = \pm L$ at progressively shorter times and the MSD saturates earlier, figure 11. Simultaneously, for more superdiffusive SBMs the spread of $\overline{\delta^2}$ traces around their ensemble mean gets smaller for the same degree of confinement, compare figure 11. Similar to confined HDPs in [35] and confined GDPs above, for hard wall-confined SBM we then have $\langle x^2 \rangle_{\text{st}} = \langle \overline{\delta^2} \rangle_{\text{st}} / 2$ due to the geometric definition (4). Therefore, the second ergodicity breaking parameter—after the initial scaling $\mathcal{EB}(\Delta) \sim (\Delta/T)^{1-(1+\beta)}$ —in the limit of long diffusion times approaches $\mathcal{EB} \rightarrow 2$, see figure 12. These behaviours are similar to those for confined GDPs presented in figure 6(b).

4. Discussion and outlook

We studied the non-homogeneous and non-stationary generalized diffusion process with the power-law diffusivity $D(x, t) \sim |x|^\alpha t^\beta$. We explored analytically and by extensive computer simulations the competition between the two parent processes revealing a number of universal characteristics. While the general scaling forms for the ensemble and time averaged MSDs are similar to those of the parent processes HDP and SBM—and in fact to those of subdiffusive continuous time random walks [4, 47, 48]—we showed that for those combinations of the scaling exponents α and β which produce a unity anomalous diffusion exponent, $\kappa = 1$, the non-stationary character of the GDP is still

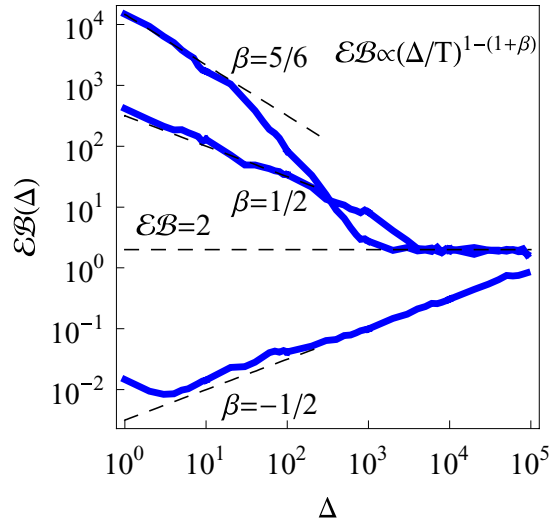


Figure 12. Auxiliary ergodicity breaking parameter for confined SBM, plotted for the parameters of figure 11.

visible in the irreproducibility of the time averaged MSD. For the ageing GDP we obtained that the ageing factor has the same functional form as for HDP, SBM, and subdiffusive continuous time random walks [4,35,42]. We also explored the properties of GDPs confined in an interval including the saturation of the MSD and the variation of the ergodicity breaking parameter with the trace length and the degree of confinement. Physically, the combination of temporal and spatial variations of the local diffusivity appears both a natural and attractive concept to model anomalous diffusion, for instance, in microscopic biological systems.

Restricted diffusion in various porous media was considered in terms of effective time dependent diffusivities. Such approaches may provide some information about the typical size of restricted regions or cavities experienced by a tracer. The concept of time dependent diffusivities is, for instance, applied to interpret signals in NMR experiments [67–69] aimed at determining the degree of tissue interconnectivity and permeability. Water and ion diffusion in various human tissues is often anisotropic and sometimes anomalous [70]. Anisotropies in water diffusion were observed in biological tissues with a directional/fibrous structure, for instance, in the white matter of the human brain, nerve fibres, and muscle fibres [68].

Specifically, the instantaneous diffusivity $D(t) = d\langle \mathbf{r}^2(t) \rangle / (6dt)$ in muscle fibres was shown to assume the long-time limit to decay $D(t) = D(\infty) + \text{const}/t^{1/2}$. Alternative power-law scaling of the form $D(t) \sim t^{-\mu}$ corresponding to different structures of the disorder in the system were also examined, μ often ranging in the interval $1/2 < \mu < 3/2$ [68]. The value of $\mu = 3/2$ is known for a fully uncorrelated medium in three dimensions. In a biological context, the power μ of the tail of the diffusivity depends on the positioning of boundaries in the system. The latter are typically cell membranes that are only weakly permeable to water or ions. It was argued that some deceases may caused changes in the brain or muscle tissues that can in principle be detected by measuring the changes in the long time diffusivity $D(\infty)$ and the exponent μ as compared to healthy

tissues. Note that in these biological examples with time-dependent diffusivity no complete localization of particles in the long-time limit exists and the basal diffusivity $D(\infty)$ is finite. To the best of our knowledge [68] represents the first attempt to assign a time dependent diffusivity to transport in tissues starting from microscopic principles.

In porous interconnected media, for instance, in a suspension of reflecting spheres [71], the long-time diffusivity of a tracer can be defined as $\bar{D}(t) = \langle \mathbf{r}^2(t) \rangle / (6t)$. It can again be represented in the time dependent form $\bar{D}(t)/D_0 \sim A_1 + A_2/t + A_3/t^{3/2}$ [72]. The leading time dependence for the instantaneous diffusion coefficient is then $D(t)/D_0 \sim A_1 - 0.5A_3t^{-3/2}$. Here $1/A_1$ is the tortuosity of the medium that renormalizes the long-time tracer diffusivity due to the presence of inter-connected cavities [71].

Are such assumptions of an effective, time dependent diffusivity always justified? In fact, any anomalous diffusion law (1) can be interpreted in terms of the effective diffusivity $K_{\text{eff}}(t) \simeq t^{1-\alpha}$, such that we can rewrite equation (1) in the form $\langle x^2(t) \rangle \simeq K_{\text{eff}}(t)t$. However, this is not sufficient to identify the observation of anomalous diffusion with the GDP or SBM models studied here. It is important to either have more detailed knowledge of the underlying physical process, which may support the GDP approach or rather other physical models such as continuous time random walks [4, 48]. In particular, we note that despite many close similarities, SBM and fractional Brownian motion (FBM) capture physically strongly different situations. If direct physical insight is not possible, the stochastic properties of the process need to be scrutinized in more detail by using complementary diagnostic tools [4, 64, 73].

Similar to these examples, position dependent diffusivities were explored in a range of systems including tracer diffusion in groundwater aquifers [7]. The position dependence is directly accessible experimentally and was systematically sampled for the motion of smaller protein tracers in living biological cells [30].

We note that HDP and SBM processes may also give rise to ultraslow diffusion with a logarithmic dependence of the MSD. For the HDP this corresponds to an exponential variation of the diffusivity in space [33] while for SBM ultraslow motion emerges in the limit $\beta \rightarrow -1$ [43]. Such ultraslow diffusion is equally weakly non-ergodic and ageing, in analogy to diffusion in ageing environments [60], diffusion in quenched Sinai disorder [59], or many particle systems with scale free time evolution [61].

Acknowledgments

We acknowledge funding from the Academy of Finland (FiDiPro scheme to RM) and the Deutsche Forschungsgemeinschaft (Grant CH 707/5-1 to AGC).

References

- [1] Bouchaud J-P and Georges A 1990 *Phys. Rep.* **195** 127
- [2] Metzler R and Klafter J 2000 *Phys. Rep.* **339** 1
Metzler R and Klafter J 2004 *J. Phys. A* **37** R161
- [3] Havlin S and Ben-Avraham D 2002 *Adv. Phys.* **51** 187
- [4] Metzler R, Jeon J-H, Cherstvy A G and Barkai E 2014 *Phys. Chem. Chem. Phys.* **16** 24128
- [5] Richardson L F 1926 *Proc. R. Soc. A* **110** 709

- [6] Solomon T H, Weeks E R and Swinney H L 1993 *Phys. Rev. Lett.* **71** 3975
Zaslavsky G M 2002 *Phys. Rep.* **371** 461 (compare the theoretical work)
Zaslavsky G M 2005 *Hamiltonian Chaos and Fractional Dynamics* (Oxford: Oxford University Press)
- [7] Haggerty R and Gorelick S M 1995 *Water Resources Res.* **31** 2383
Scher H, Margolin G, Metzler R, Klafter J and Berkowitz B 2002 *Geophys. Res. Lett.* **29** 1061
Berkowitz B, Cortis A, Dentz M and H Scher 2006 *Rev. Geophys.* **44** RG2003
- [8] Scher H and Montroll E W 1975 *Phys. Rev. B* **12** 2455
- [9] Schubert M *et al* 2013 *Phys. Rev. B* **87** 024203
- [10] Rigler R and Elson E S 2011 *Fluorescence Correlation Spectroscopy: Theory and Applications* (Berlin: Springer)
- [11] Bräuchle C, Lamb D C and Michaelis J 2012 *Single Particle Tracking and Single Molecule Energy Transfer* (New York: Wiley)
Xie X S, Choi P J, Li G-W, Lee N K and Lia G 2008 *Annu. Rev. Biophys.* **37** 417
- [12] Wong I Y, Gardel M L, Reichman D R, Weeks E R, Valentine M T, Bausch A R and Weitz D A 2004 *Phys. Rev. Lett.* **92** 178101
- [13] Mattsson J, Wyss H M, Fernandez-Nieves A, Miyazaki K, Hu Z B, Reichman D R and Weitz D A 2009 *Nature* **462** 83
Zhou E H, Trepats X, Park C Y, Lenormand G, Oliver M N, Mijalovich S M, Hardin C, Weitz D A, Butler J P and Fredberg J J 2009 *Proc. Natl Acad. Sci.* **106** 10632
Fierro A, del Gado E, de Candia A and Coniglio A 2008 *J. Stat. Mech.* **L04002**
- [14] Szymanski J and Weiss M 2009 *Phys. Rev. Lett.* **103** 038102
Guigas G, Kalla C and Weiss M 2007 *Biophys. J.* **93** 316
Pan W, Filobelo L, Pham N D Q, Galkin O, Uzunova V V and Vekilov P G 2009 *Phys. Rev. Lett.* **102** 058101
- [15] Jeon J-H, Leijnse N, Oddershede L B and Metzler R 2013 *New J. Phys.* **15** 045011
- [16] Robert D, Nguyen T H, Gallet F and Wilhelm C 2010 *PLoS ONE* **4** e10046
Jeon J-H, Tejedor V, Burov S, Barkai E, Selhuber-Unkel C, Berg-Sørensen K, Oddershede L and Metzler R 2011 *Phys. Rev. Lett.* **106** 048103
Bronstein I, Israel Y, Kepten E, Mai S, Shav-Tal Y, Barkai E and Garini Y 2009 *Phys. Rev. Lett.* **103** 018102
Golding I and Cox E C 2006 *Phys. Rev. Lett.* **96** 098102
- [17] Weigel A V, Simon B, Tamkun M M and Krapf D 2011 *Proc. Natl Acad. Sci. USA* **108** 6438
Tabei S M A, Burov S, Kim H Y, Kuznetsov A, Huynh T, Jureller J, Philipson L H, Dinner A R and Scherer N F 2013 *Proc. Natl Acad. Sci. USA* **110** 4911
- [18] Höfling F and Franosch T 2013 *Rep. Prog. Phys.* **76** 046602
Saxton M J and Jacobsen K 1997 *Ann. Rev. Biophys. Biomol. Struct.* **26** 373
- [19] Godec A, Bauer M and Metzler R 2014 *New J. Phys.* **16** 092002
Lee C H, Crosby A J, Emrick T and Hayward R C 2014 *Macromolecules* **47** 741 (compare the experiments)
- [20] Kneller G R, Baczynski K and Pasienkewicz-Gierula M 2011 *J. Chem. Phys.* **135** 141105
Jeon J-H, Martinez-Seara Monne H, Javanainen M and Metzler R 2012 *Phys. Rev. Lett.* **109** 188103
- [21] Spanner M, Höfling F, Schröder-Turk G E, Mecke K and Franosch T 2011 *J. Phys. Condens. Matter* **23** 234120
Klemm A, Metzler R and Kimmich R 2002 *Phys. Rev. E* **65** 021112
Klemm A and Kimmich R 1997 *Phys. Rev. E* **55** 4413
- [22] Höfling F and Franosch T 2007 *Phys. Rev. Lett.* **98** 140601
Leitmann S and Franosch T 2013 *Phys. Rev. Lett.* **111** 190603
Barkai E, Fleurov V and Klafter J 2000 *Phys. Rev. E* **61** 1164
- [23] Montroll E W and Weiss G H 1965 *J. Math. Phys.* **6** 167
- [24] Bertin E and Bouchaud J-P 2003 *Phys. Rev. E* **67** 026128
Monthus C and Bouchaud J-P 1996 *J. Phys. A* **29** 3847
Burov S and Barkai E 2007 *Phys. Rev. Lett.* **98** 250601
- [25] Mandelbrot B B and van Ness J W 1968 *SIAM Rev.* **10** 422
Mandelbrot B B and van Ness J W 1965 *C. R. Acad. Sci.* **260** 3274 (compare also)
- [26] Kneller G 2014 *J. Chem. Phys.* **141** 041105
Goychuk I 2009 *Phys. Rev. E* **80** 046125
Goychuk I 2012 *Adv. Chem. Phys.* **150** 187
- [27] Taloni A, Chechkin A V and Klafter J 2010 *Phys. Rev. Lett.* **104** 160602
Taloni A, Chechkin A V and Klafter J 2012 *Europhys. Lett.* **97** 30001
- [28] Panja D 2010 *J. Stat. Mech.* **L02001**
Panja D 2010 *J. Stat. Mech.* **P06011**

- [29] Taloni A and Lomholt M A 2008 *Phys. Rev. E* **78** 051116
Lizana L, Ambjörnsson T, Taloni A, Barkai E and Lomholt M 2010 *Phys. Rev. E* **81** 051118
- [30] Kühn T, Ihalainen T O, Hyväluoma J, Dross N, Willman S F, Langowski J, Vihinen-Ranta M and Timonen J 2011 *PLoS One* **6** e22962
English B P, Hauryliuk V, Sanamrad A, Tankov S, Dekker N H and Elf J 2011 *Proc. Natl Acad. Sci.* **108** E365
- [31] Fuliński A 2011 *Phys. Rev. E* **83** 061140
Fuliński A 2013 *J. Chem. Phys.* **138** 021101
Fuliński A 2013 *Acta Phys. Pol.* **44** 1137
- [32] Cherstvy A G, Chechkin A V and Metzler R 2013 *New J. Phys.* **15** 083039
- [33] Cherstvy A G and Metzler R 2013 *Phys. Chem. Chem. Phys.* **15** 20220
- [34] Cherstvy A G, Chechkin A V and Metzler R 2014 *Soft Matter* **10** 1591
- [35] Cherstvy A G and Metzler R 2014 *Phys. Rev. E* **90** 012134
Cherstvy A G, Chechkin A V and Metzler R 2014 *J. Phys. A* **47** 485002
Cherstvy A G and Metzler R 2015 *J. Chem. Phys.* **142** 144105
- [36] Massignan P, Manzo C, Torreno-Pina J A, García-Parako M F, Lewenstein M and Lapeyre G L Jr 2014 *Phys. Rev. Lett.* **112** 150603
- [37] Batchelor G K 1952 *Math. Proc. Camb. Phil. Soc.* **48** 345
- [38] Saxton M J 2001 *Biophys. J.* **81** 2226
Guigas G, Kalla C and Weiss M 2007 *FEBS Lett.* **581** 5094
Periasmy N and Verkman A S 1998 *Biophys. J.* **75** 557
Latour L L, Svoboda K, Mitra P and Sotak C H 1994 *Proc. Natl Acad. Sci. USA* **91** 1229
Wu J and Berland M 2008 *Biophys. J.* **95** 2049
Szymanski J, Patkowski A, Gapiski J, Wilk A and Holyst R 2006 *J. Phys. Chem. B* **110** 7367
Lutsko J F and Boon J P 2013 *Phys. Rev. Lett.* **88** 022108
- [39] Lim S C and Muniandy S V 2002 *Phys. Rev. E* **66** 021114
- [40] Thiel F and Sokolov I M 2014 *Phys. Rev. E* **89** 012115
- [41] Jeon J-H, Chechkin A V and Metzler R 2014 *Phys. Chem. Chem. Phys.* **16** 15811
- [42] Safdari H, Chechkin A V, Jafari G R and Metzler R 2015 *Phys. Rev.* **91** 042107
- [43] Bodrova A, Chechkin A G, Cherstvy A V and Metzler R e-print arXiv:1503.08125
- [44] Bodrova A, Chechkin A V, Cherstvy A G and Metzler R e-print arXiv:1501.04173
- [45] Platani M, Goldberg I, Lamond A I and Swedlow J R 2002 *Nat. Cell Biol.* **4** 502
- [46] Okubo A 1962 *J. Oceanol. Soc. Japan* **20** 286
Hentschel H G E and Procaccia I 1984 *Phys. Rev. A* **29** 1461
- [47] Burov S, Jeon J-H, Metzler R and Barkai E 2011 *Phys. Chem. Chem. Phys.* **13** 1800
- [48] Barkai E, Garini Y and Metzler R 2012 *Phys. Today* **65** 29
- [49] Sokolov I M 2012 *Soft Matter* **8** 9043
- [50] Reichl L 2009 *A Modern Course in Statistical Physics* (New York: Wiley)
Toda M, Kubo R and Saitō N 1992 *Statistical Physics I: Equilibrium Statistical Mechanics* (Berlin: Springer)
Khinchin A Y 2003 *Mathematical Foundations of Statistical Mechanics* (New York: Dover)
- [51] Deng W and Barkai E 2009 *Phys. Rev. E* **79** 011112
- [52] Jeon J-H and Metzler R 2010 *J. Phys. A* **43** 252001
Jeon J-H and Metzler R 2012 *Phys. Rev. E* **85** 021147
- [53] Jeon J-H and Metzler R 2012 *Phys. Rev. E* **85** 021147
Kursawe J, Schulz J H P and Metzler R 2013 *Phys. Rev. E* **88** 062124
- [54] Meroz Y, Sokolov I M and Klafter J 2010 *Phys. Rev. E* **81** 010101
- [55] Burov S, Metzler R and Barkai E 2010 *Proc. Natl Acad. Sci. USA* **107** 13228
- [56] Bouchaud J-P 1992 *J. Phys. I* **2** 1705
Bel G and Barkai E 2005 *Phys. Rev. Lett.* **94** 240602
Bel G and Barkai E 2006 *Phys. Rev. E* **73** 016125
Rebenshtok A and Barkai E 2007 *Phys. Rev. Lett.* **99** 210601
Lomholt M A, Zaid I M and Metzler R 2007 *Phys. Rev. Lett.* **98** 200603
Aquino G, Grigolini P and West B J 2007 *Europhys. Lett.* **80** 10002
- [57] Lubelski A, Sokolov I M and Klafter J 2008 *Phys. Rev. Lett.* **100** 250602
Sokolov I M, Heinsalu E, Hänggi P and Goychuk I 2010 *Europhys. Lett.* **86** 041119
Khoury M, Lacasta A M, Sancho J M and Lindenberg K 2011 *Phys. Rev. Lett.* **106** 090602
Skaug M J, Lacasta A M, Ramirez-Piscina L, Sancho J M, Lindenberg K and Schwartz D K 2014 *Soft Matter* **10** 753

- [58] He Y, Burov S, Metzler R and Barkai E 2008 *Phys. Rev. Lett.* **101** 058101
- [59] Godec A, Chechkin A V, Barkai E, Kantz H and Metzler R 2014 *J. Phys. A* **47** 492002
- [60] Lomholt M A, Lizana L, Metzler R and Ambjörnsson T 2013 *Phys. Rev. Lett.* **110** 208301
- [61] Sanders L P, Lomholt M A, Lizana L, Fogelmark K, Metzler R and Ambjörnsson T 2014 *New J. Phys.* **16** 113050
- [62] Denisov S I, Yuste S B, Bystrik Yu S, Kantz H and Lindenberg K 2011 *Phys. Rev. E* **84** 061143
- [63] Godec A and Metzler R 2013 *Phys. Rev. Lett.* **110** 020603
- [64] Magdziarz M, Weron A, Burnecki K and Klafter J 2009 *Phys. Rev. Lett.* **103** 180602
- [65] Jeon J-H, Barkai E and Metzler R 2013 *J. Chem. Phys.* **139** 121916
- [66] Schulz J H P, Barkai E and Metzler R 2013 *Phys. Rev. Lett.* **110** 020602
Schulz J H P, Barkai E and Metzler R 2014 *Phys. Rev. X* **4** 011028
- [67] Novikov D S, Fieremans E, Jensen J H and Helpert J A 2011 *Nat. Phys.* **7** 508
- [68] Novikov D S, Jensen J H, Helpert J A and Fieremans E 2014 *Proc. Natl Acad. Sci. U.S.A.* **111** 5088
- [69] Grebenkov D S 2007 *Rev. Mod. Phys.* **79** 1077
- [70] Sykova E and Nicholson C 2008 *Physiol. Rev.* **88** 1277
- [71] de Swiet T M and Sen P N 1996 *J. Chem. Phys.* **104** 206
Sen P N 2004 *Concepts Magn. Reson. A* **23** 1
- [72] Loskutov V V 2012 *J. Magn. Reson.* **216** 192
Loskutov V V and Sevriugin V A 2013 *J. Magn. Reson.* **230** 1
Erdel F, Baum M and Rippe K 2015 *J. Phys.: Condens. Matter* **27** 064115
- [73] Tejedor V, Benichou O, Voituriez R, Jungmann R, Simmel F, Selhuber-Unkel C, Oddershede L and Metzler R 2010 *Biophys. J.* **98** 1364
O'Malley D, Vesselinov V V and Cushman J H 2014 *J. Stat. Phys.* **156** 896
Robson A, Burrage K and Leake M C 2012 *Phil. Trans. R. Soc. B* **368** 20120029
Krüsemann H, Godec A and Metzler R 2014 *Phys. Rev. E* **89** 040101
Condamin S, Tejedor V, Voituriez R, Bénichou O and Klafter J 2008 *Proc. Natl Acad. Sci.* **105** 5675
Meroz Y and Sokolov I M 2015 *Phys. Rep.* **573** 1